FUTURE CITIES AND ENVIRONMENT

New Technologies in the Processing of European Digital Heritage and Their Application to the Historical Images of the American Flight of 1944 Over Spain

TECHNICAL ARTICLE

JUAN-LUIS BERMÚDEZ-GONZÁLEZ
ENRIQUE FERNÁNDEZ TAPIA
ENRIQUE CASTAÑO PEREA
*Author affiliations can be found in the back matter of this article

ubiquity press

ABSTRACT

Historical aerial images constitute an invaluable heritage that requires meticulous recovery and preservation. Interest in this task has been shown at the international level, where several congresses have been held to analyse orthophotographs production techniques, as well as the state of the art of preservation and dissemination of historical material. Innovative image orthorectification models, such as Structure for Motion and Multi-View Stereo, derived from classical photogrammetric methods such as collinearity equations, Direct Linear Transformation and Rational Function Model, have shown excellent results in the creation of 3D models from images captured by mobile devices and unmanned aerial vehicles (UAVs). These advances open up a new line of research for its application in historical flights, characterised by unsuitable flight and conservation conditions, with geometries away from the conventional geometric model and the absence of orientation parameters. On the basis of the papers presented at the EuroSDR congresses in 2019 and 2022, and using SfM and MVS algorithmic programmes, research on the processes of orthorectification of historical images has been deepened, particularly in the processing of large volumes of data. The methodology was applied to what is potentially the largest block of data to date, comprising over 4,000 images covering an area of over 40,000 square kilometres corresponding to the A-series flight, carried out by the US Army Map Service between 1945 and 1946. This technical process represents a significant step towards the accurate correction of valuable historical aerial imagery, contributing to architectural study, urban planning, property organisation, and historical heritage conservation.

CORRESPONDING AUTHOR:
Juan-Luis Bermúdez-González
Department of Architecture, University of Alcalá (UAH), Spain
luis.bermudez@uah.es

KEYWORDS:
Historical images; Digital heritage; Aerial photogrammetry; Orthorectification; SfM

TO CITE THIS ARTICLE:
Bermúdez-González, J-L, Fernández Tapia, E and Castaño Perea, E. 2024. New Technologies in the Processing of European Digital Heritage and Their Application to the Historical Images of the American Flight of 1944 Over Spain. *Future Cities and Environment,* 10(1): 13, 1–15. DOI: https://doi.org/10.5334/fce.252

1. INTRODUCTION

Historical images and old photographs, which capture a specific portion of space at a specific time, are crucial for the knowledge of history, urban evolution, and heritage conservation over time (Condorelli & Morena 2023). For this reason, more and more countries are digitising or have digitised their aerial image archives (Giordano & Mallet 2019). However, automatic photogrammetric processing of historical aerial photographs remains a challenging task, especially when ancillary information is missing (Farella et al. 2022). Its application requires prior photogrammetric processes that are often limited by technical constraints, such as the lack of information on Ground Control Points (GCPs) and precise camera parameters, hindering the accurate orthorectification of raw images (Pinto et al. 2019).

Although many historical flights were considered lost due to lack of preservation or economic problems for their digitisation (Quirós & Fernández 1997; Pérez et al. 2013), the high interest in this historical documentation has led many countries to digitise and process their aerial image archives. The European Spatial Data Research (EuroSDR), in its publication number 70, February 2019, included a comprehensive study on the state of archiving and processing of historical aerial images in Europe (Giordano & Mallet 2019), accompanied by a congress in Paris that year, a comparative study in 2021 and a new congress in Rome in December 2022, confirming the scientific, political and social interest in the geometric correction of historical images. The EuroSDR study was launched in 2017 with a questionnaire sent to all European member organisations of EuroSDR and EuroGeographics. According to the survey, most organisations have hundreds of thousands of historical images, with the French Institut Géographique National standing out with 4.7 million images. All organisations have implemented measures to generate orthoimagery from analogue aerial imagery. However, there is currently no unified standard, consensus, or solution. Instead, each organisation has conducted its own research and developed its own specifications.

2. RATIONALE AND OBJECTIVES

In Spain, we have an almost complete flight of the peninsular territory with a very high spatial resolution and almost 80 years old: the historical aerial photographs of the American A-series flight (1945–46), that was part of the Casey Jones project for a photogrammetric flight of Western Europe carried out by the USAAF and the RAF at the end of the Second World War. The main conclusions of the EuroSDR study, directly related to the subject of this research, point to problems linked to the lack of camera calibration files, which makes it necessary to use self-calibration techniques. The difficulty and time required to search for GCPs in old analogue images is also highlighted, as well as the lack of efficient workflows and clear and beneficial use cases. Although classical methods of aerial triangulation have been successfully tested over the last century, and new mathematical models derived from collinearity equations have given excellent results for Unmanned Aerial Vehicle (UAV) photography, reducing the number of GCPs and the calibration data required for model resolution, the results of these models have yet to be analysed in depth when applied to historical imagery. The aim of this research is to continue the investigations carried out on the techniques and processes of geometric correction of historical aerial imagery by deepening on Structure for Motion (SfM) based techniques and their possible application to a large dataset.

The aim of this research is to analyse the results of photogrammetric processes on historical images obtained in recent studies by other international research teams. It will be applied to the orthorectification of the American A-series flight in the Autonomous Community of Extremadura (Spain), analysing the results obtained and using them as a basis for studies of the territory and the location of missing heritage elements being carried out by this research team. The result of the research will provide a procedure for the geometric correction of large sets of images with conical projection and unknown orientation parameters. The digitisation of these aerial images provides a dense temporal sampling of territories, allowing comparative analysis and observation of changes over decades and even over the last 120 years. This is especially useful for studies on land use changes, urban evolution, deforestation, coastline modifications and other geographical and environmental phenomena (Heisig, Jörg & Streilein 2019).

3. BACKGROUND ON MATHEMATICAL MODELS FOR IMAGE CORRECTION

Three types of solutions can be distinguished for image georectification: Analytical, parametric, and non-parametric (Figure 1).

3.1 ANALYTICAL MODELS

Analytical methods, or direct correction methods, are solutions that do not take into account the camera or the geometry of the photographic image. Polynomial rectification of the image is the simplest and is the method usually used by CAD systems, the quality of the results being highly conditioned by the input data. This function attempts to correct, by deforming the image, the effects of relief, camera distortion, terrestrial curvature, etc... based on the points measured on the ground. Therefore, it is a method that is not valid, except for slightly pronounced relief and cameras without distortion, as it would require

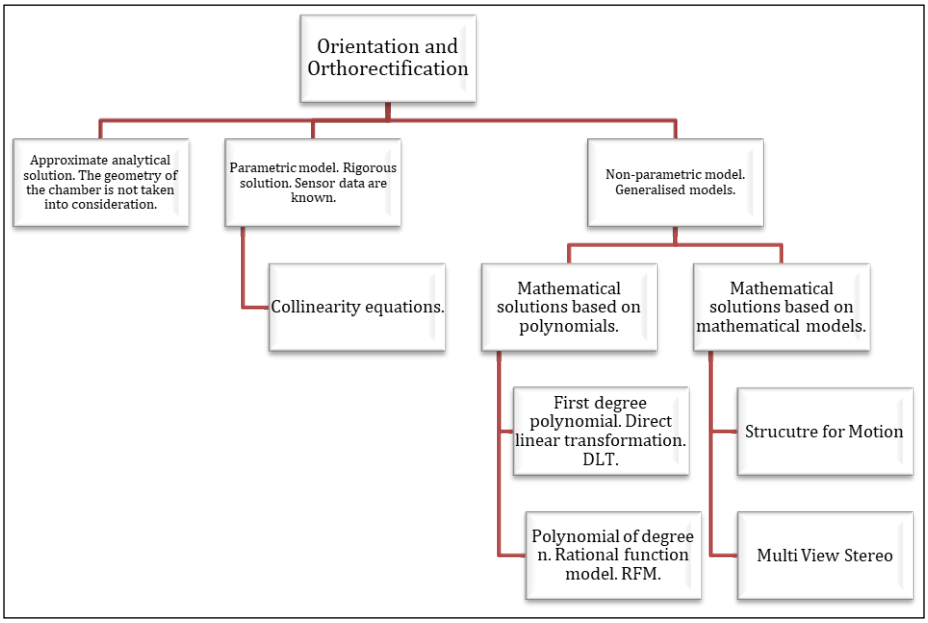

Figure 1 Classification of orientation and orthorectification methods.

an infinite number of points to produce an acceptable correction model. In terrestrial photogrammetry applied to architecture, methods such as unwrapping have been used, where the Digital Surface Model (DSM) is replaced by a known mathematical surface, a plane, a cone, or a cylinder (Hemmleb & Wiedemann 1997). Although it can provide satisfactory results on simple architectural facades and can be useful in the case of orthorectification of images of missing buildings, where it is not possible to generate a DSM, it has no application in the case of more complex elements or aerial photography.

On the other hand, there are photogrammetric methods that take into account the position and orientation of the camera as well as its internal geometry, which allows them to be classified into parametric and non-parametric models, depending on whether the camera data are known or mathematically modelled, although this distinction is sometimes blurred or confused by the allusion to the parameters of the equations themselves in non-parametric models.

3.2 PARAMETRIC MODELS. PHYSICAL MODELS

The differential rectification method is the one currently used in the creation of orthophotographs, considered the best method because it allows correcting all the distortions caused by the sensor, in addition to those caused by the projection and the terrain (Temiz 2008). Mathematically, orthorectification using analytical aerial triangulation methods, through the application of collinearity equations and two-dimensional projective transformation, is part of the so-called parametric approach. This is a mathematically rigorous solution in which the camera orientation data must be known, as it utilises the collinearity conditions of the central perspective, a digital surface model (DSM), and the ground control points (GCPs) to create a reversible object-image transformation (Guoqing et al. 2002) and obtain the new XY coordinates of the image pixel based on the location of the XYZ centre of projection, the orientation of the perspective beam, and the elevation of the Z point on the ground, for that same planimetric position. When the internal geometry of the camera is known, the model is then called a rigorous model or physical model, because it uses the physical sensor data, while models in which camera data are calculated from other data are called generalised or non-parametric models.

3.3 NON-PARAMETRIC MODELS

Generalised sensor models have reduced the need to obtain a physical sensor model, and with it, the requirement for a comprehensive understanding of the camera parameters. In a generalised sensor model, the transformation between image and object space is represented as a general function without modelling the physical imaging process. The function can take different forms, such as polynomials or rational functions. The use of the generalised sensor model as a replacement for the physical sensor model for real-time photogrammetric processing is a logical choice, provided that the decrease in accuracy is negligible (Paderes, Mikhail & Fagerman 1989; Tao & Hu 2001a). Another advantage is the ease with which different cameras can be modelled at the computer level, simply by changing the values of the coefficients in the generalised sensor model (Tao & Hu 2001b).

The Direct Linear Transformation (DLT) model is a modelling with a larger number of parameters of the rigorous model, where the exterior orientation parameters are included to determine the relationship between GCPs and their image, so it is necessary to have GCPs to be able to apply the method. Thus, the collinearity

condition, commonly used in rigorous camera models, is essentially a special expression of the DLT, a different expression from the rigorous camera model represented by the collinearity condition and its parameters, which was developed by Abdel-Aziz and Karara in the early 1970s, and which can be used, instead of a rigorous camera model, to represent the image geometry in the geometrical correction process (Ma & Buchwald 2012; Remondino 2022). Compared to a rigorous camera model, which uses eight parameters, the DLT model uses three more parameters to represent the image geometry.

However, in the case of historical aerial photographs, the camera calibration data are often absent or difficult to determine and obtaining these parameters using the classical DLT equations, from measured GCPs, is impractical due to the difficulty of having a large set of highly accurate and properly distributed. In these cases, Rational Function Models (RFM) are used, calculated from GCPs. However, as Ma points out (Ma & Buchwald 2012), there is numerous literature indicating that RFM can be employed without knowing the camera orientation parameters. In addition to this, as the RFM sensor model implicitly provides the inner and outer orientation of the sensor, the availability of GCPs is no longer a mandatory requirement and, consequently, the use of RFM for photogrammetric mapping is becoming a new standard in high-resolution satellite imagery. The RFM sensor model describes the geometric relationship between object space and image space. It relates the coordinates of the object points (X,Y,Z) to the coordinates of the image pixels (r,c) or vice versa using 78 Rational Polynomial Coefficients (RPCs) (Okeke 2010).

When the physical sensor parameters are known, the RFM is basically solved using these parameters, the accuracy then depends on the physical sensor and not on the GCPs. This is known as the terrain-independent solution. However, the geometric accuracies obtained in this way in the sensor orientation phase are not particularly good. An interesting possibility of this method is that the user can improve this initial accuracy by refining the rational coefficients by introducing some GCPs in the model, even in the absence of a physical sensor model, the RFM can be solved using only terrain control points, and in this case the quality of the solution depends on the number of points, their quality and distribution, and is therefore referred to as terrain-dependent solution model (Tao & Hu 2001a).

The last approach would be the Structure for Motion (SfM) models, sometimes called Visual Structure for Motion (VSfM), which are applied by state-of-the-art photogrammetry software. These algorithms have been designed initially for the reconstruction of three-dimensional objects from moving photographs from uncalibrated cameras, such as those taken from mobile phones and unmanned aerial vehicles. The type of camera motion, unlike classical models, is not a uniform rectilinear motion, nor do the photographs have parallel shooting axes, but could be defined as a non-predefined motion along the object, with shooting axes that can be convergent. SfM is concerned with reconstructing the three-dimensional structure of an object or scene and estimating camera motion parameters from multiple views of the scene. The goal is to determine both the 3D layout of the points and the camera trajectory over time. RFM-based camera calibration techniques are used to understand the relationship between the coordinates of the 3D points and their projections in the images, whereas 3D motion, and structure estimation methods are applied in SfM to infer the spatial arrangement of points and camera trajectory from observations in multiple images. For the last, the Multi-View Stereo (MVS) is the technique that allows the creation of a dense point cloud from the data provided by the SfM model. In other words, Multi-View Stereo photogrammetry uses several images simultaneously, unlike classical models which only use images in pairs.

4. STATE OF THE ART IN GEOMETRIC CORRECTION OF HISTORICAL IMAGES

The casuistry of historical flights is so wide that it is very difficult to carry out a study of results only from a theoretical point of view, since the methodology and accuracy cannot be established, at a general level, for each type of camera, scale or pixel size, being more appropriate to speak of specific accuracy for each processed dataset and even for each of the sub-blocks generated within the dataset. For this reason, the state of the art in the theoretical development of the issue, which has already been analysed above, has not been studied in depth, but rather the state of the art in image correction methods is analysed through the evaluation of practical cases, trying to find points in common between the different experiences.

The Swiss Confederation has used the PCI Geomatica software, making use of the HAP (Historical Air Photo) module (Heisig, Jörg & Streilein 2019). The main difficulties they pointed out were the unknown focal length of the camera and the absence of fiducial marks, and the solution applied was to establish new fiducial marks using the corners of the photographic plate. As far as the aerial triangulation blocks were concerned, they opted for blocks of 300 to 400 images, with 9 to 10 passes of 35 to 45 images per pass, and a total of 14 blocks for the entire national territory. The method used for ground support was the assignment of manual points, for a previous orientation, and a subsequent process of automatic detection of control points, based on correlation with a current reference orthoimage. The distribution of manual control points, although irregular, has been the classic one in aerial triangulation blocks, central area and in the corners of the blocks, although a redundancy of points in certain areas can be clearly

seen, probably placed a posteriori, in order to improve the results in these areas.

It can be seen that the residuals of the manual control points were high, but the very high number of automatic control points minimised the overall error, from a statistical point of view. The mean squared errors obtained at the control points, for a typical block, are 11 pixels on the X axis and 13 pixels on the Y axis. With a scanning resolution of 14 microns, this equates to 5 metres along the X axis, 9.5 metres along the Y axis, and 8 metres along the Z axis.

The results of the application of the DLT model by Ma and Buchwald (2012) to six historical 1:20,000 scale images resulted in an RMSE of 6.42 m. In this same study the authors digitize several linear elements and compares the results obtained in the direct linear transformation (DLT) model, with the SfM model and with direct georeferencing without correction, obtaining an almost perfect correspondence between the geometric solution of the DLT and the SfM, while the direct georeferencing process places the displaced linear feature an average distance of 360 meters from the previous solutions.

Tests by Ma and Buchwald (2012) on aerial photographs show that the accuracy of a first-order polynomial can give acceptable results, and some studies even suggest that second- and third-order polynomials have a worse fit than a DLT (first-order polynomial) for use in historical flights. The review of work carried out by Farella et al. (2022) on a dataset from the TIME Benchmark project, indicates an error in GCPs of 4 metres for the 1958 flight and 3.5 metres for the 1976 flight, with GSD of 0.5 and 0.2 metres for the X and Y axes respectively when a Helmert transformation is applied directly on the data for georeferencing, which is an error of 5 to 6 times the GSD, and denotes the need to apply additional corrections.

Nocerino, Menna and Remondino (2018) performed orthorectification of several historical images from World War II aerial reconnaissance flights, possibly taken with a Fairchild K-17, with 20 cm GSD and supported by a 1 m spatial resolution MDS. The RMSE obtained for three different blocks of 2, 5, and 6 images with an average flight height of 7,550 m, was between two and three times the a priori error, reaching 2.5 m in planimetry and 9 m in altimetry. DLT was used to process the images, and the final error is higher than initially estimated, probably due to the configuration of the block in a single pass, with a longitudinal overlap of less than 60% in some cases. Although some studies indicate that an inappropriate block configuration can be compensated by adding additional parameters to correct for both lens geometric errors and other possible geometric distortions (Redecker 2008; Redweik et al. 2009), in this case, possibly due to the huge focal length used in the flight (609.6 mm) the results do not improve even if the number of GCPs is increased, because the geometry at the intersection of homologous rays is very unstable, and very strong adjustment can reduce the RMSE but cause distortion of the orthophotography, with consequent loss of quality. This fact can be observed in Ma (2013), where the use of RFM shows that the fitting errors, in terms of the RMSE of the control point, generally decrease as the degree of the polynomial increases. However, the slight increase in accuracy does not always compensate for the risk involved, as higher order SfM requires accurate and well distributed control points, otherwise asymptotic surfaces may exist within the ground coverage of an image, leading to large distortions, as the same author points out.

Pinto et al. (2019) in orthorectification tests using DLT uses a program developed by his research team that implements DLT on historical images through a workflow they call HAPO, historical aerial photographs orthorectification. The images used in the project have a scale of 1:29,500 and a scanned pixel size of 21 microns, which gives a GSD of approximately 0.62 metres, and lack a camera calibration certificate. The results had an average error in the control points of 1.97 m.

On the other hand, Ma et al. (2020) uses SfM techniques for orthorectification of historical images with a GSD of 0.3 metres, in which the average reprojection error is only 0.2 metres, which the author points out is an abnormally low value that is probably due to the small base-to-height ratio that makes large errors in image space undetectable in the field. The same authors point out that, although the images come from a single camera, the scanning processes inevitably cause the resulting images to have different orientations in relation to the original photographs. This implies the displacement of the main camera point, obviously, not with respect to the fiducial centre, but to the pixel coordinate origin of the image, which is the origin to be used in digital image photogrammetry if we do not measure the fiducial marks manually. Theoretically, when using SfM, it is possible to have different camera models for each scanned photograph, provided a large number of control points are available. However, this is not advisable as it would drastically increase the complexity of the problem and could cause the system of equations not to converge, so Ma et al. opted to standardise the number of rows and columns of the images, arbitrarily choosing 10,844 by 8,500 pixels, and then perform a measurement of the fiducial marks, calculating the affine transformation that relates both pixel/fiducial coordinate systems. On the other hand, it indicates that the positional quality of the orthophotographs depends directly on the quality of the MDS used and, having used an MDS from the dense model calculated in the process, in which the author found significant errors, it is possible that the errors in the control points are due to the MDS. These errors in the points on the orthophotography resulted in values above the expected values, most of them below 10 m, 25% between 10 and 20 m and 10% with errors above 20 m. For this reason, the authors decided to increase the number

of GCPs from the initial 34 to 74 points and, again, the result was not as expected, as the calculated geometry was very stable with no variation in the orthophotographs produced or in the position of the points.

Another example is given by the Swedish Mapping, Cadastral and Alna Registration Authority, which digitised the images of the historic flights with a pixel size of 0.5 m. The processes of orientation, orthorectification and mosaicking were carried out semi-automatically, with occasional support from specialised personnel to adjust the results, which enabled them to achieve an RMS of 1.3 m. in X and 0.9 m. in Y for the 1960 flight, and 1 m. and 0.9 m. in XY for the 1975 flight.

At the EuroSDR 2019 conference, Meixner (2019) presented the results of their work on 11,000 1975 images of the Lombardy region, using the current MDS with a 20 m grid spacing, with CGPs extracted from the 2012 RGB orthophotography, with a GSD of 50 centimetres, with the aim of realising historical orthoimages with a GSD of 30 cm. The project is divided into 17 aerial triangulation blocks, with an average of about 600 photos per block. Camera calibration data was available. Some control points were measured manually and then a process of point measurement and block adjustment was carried out using ISAT, resulting in an RMS of 1.3 m in planimetry and 1.5 m in altimetry. From the analysis of the data it can be deduced that the number of points used for the altimetric control is 1.5 times the number of points used for the XY control, with the ratio becoming greater, reaching 1:1.8 the larger the block size, but the relationship between the number of GCPs and the block size is inverse, the larger the block size, the smaller the proportional number of GCP, in a ratio that varies from 1 point in planimetry for every 7 photos to 1:12. With this configuration, there is no correlation between the size of the photos in the block and the RMS.

Finally, the French Institut Géographique National (Giordano & Le Bris 2019) presents a procedure for the automated treatment of orthorectification processes of historical images using the self-developed program MicMac on images of different years. As in the previous cases, there is a correlation between the RMS in X and Y, but, curiously, the RMS in Z is at lower values than the RMS in planimetry, between 1 and 2 times lower. On the other hand, the analysis of the published data confirms a known fact, which is the direct relationship between the pixel size and the RMS on the GCP, but it is surprising to observe that the GSD:RSM ratio does not remain constant, but the RSM increases when we reduce the pixel size, which shows that in historical flights the influence of external elements is so high that a reduction in the GSD does not directly affect the RMS values, varying the GSD:RSM ratio from 1:7 in GSD values of 0.11 metres, to 1:3.5 for a GSD of 0.66 metres.

5. METHODOLOGICAL APPLICATION TO THE CASE OF THE 1945 AMERICAN FLIGHT OVER EXTREMADURA

After the analysis of procedures, problems and results presented in previous research, a working methodology is established for the elaboration of the historical orthophotography of Extremadura from the 1945 aerial images, carried out as part of the American flight series-A over the Iberian Peninsula. A working procedure as shown in Figure 2 is determined. The image analysis process is essential to identify the camera used to take each image, to avoid combining different cameras in the same aerial triangulation block and to analyse the problems of the images and carry out a study to propose solutions to correct them or minimise their impact on the final result. On the other hand, when selecting the GCPs it is also necessary to select the reference DSM. As the objective is to process as large a block as possible, the process is repeated until a single block with all the data is reached.

5.1 IMAGE ANALYSIS, STATUS REPORT AND CLASSIFICATION

A total of approximately 4,000 digital images were received and scanned with a ground sampling distance (GSD) of 0.43 metres, which covered an area of approximately 40,000 square kilometres. Upon analysis, it

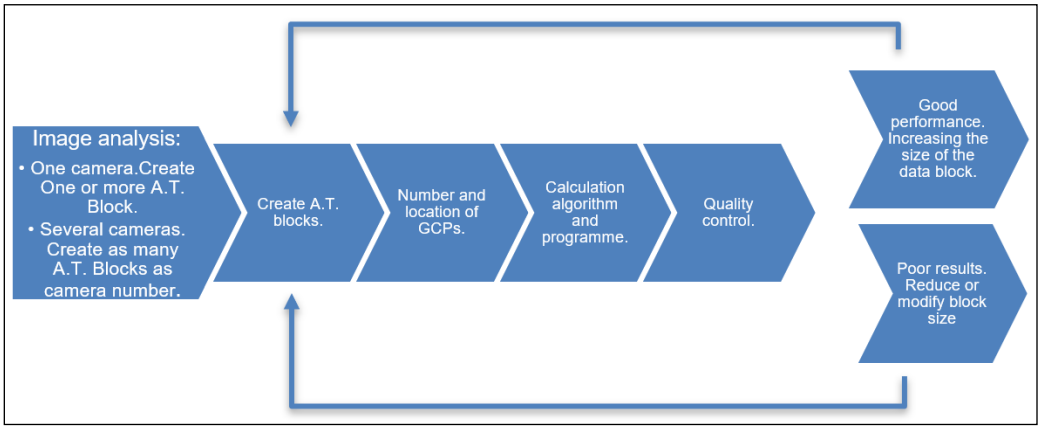

Figure 2 Classification of guidance and orthorectification methods.

was discovered that there were significant discrepancies in the digital dimensions of the files. Images with dimensions ranging from 16,368 pixels × 16,482 pixels to 25,564 pixels × 23,642 pixels were identified. However, the metadata provided indicated that the pixel size was consistent at 21 microns and that the approximate flight altitude was similar in all cases.

This would not be possible if the image had been obtained from negatives of the same dimensions, with the same scanning resolution and the same focal length for all negatives (Figure 3). Given that the pixel size in the scan is known, the only remaining possibility is that the camera format is smaller or that the focal length used was different. It has been established that the existence of a small-format Fairchild K-17 camera is unlikely, as no such camera has been identified in the historical flight archive. Consequently, a second camera, designated the Fairchild K-17 B-2, has been created to address the issue. This camera allows the system to adjust the parameters independently for the two cameras, either by using a different focal length or by using a different focal length, either using a different focal length or a larger pixel size than indicated in the metadata. This can be deduced from the relationship between focal length, flight altitude, image size (pixels) and ground surface (GSD).

The second issue identified with the provided images is their format, which is Enhanced Compressed Wavelet (ECW). This format is a lossy image storage system, which means that after the negatives were scanned, there was a loss of quality in the digital image when it was transformed from RAW or TIF format to ECW. Although ECW is a highly effective compression method, based on the elimination of high-frequency details in the image, and that it allows the user to choose the compression level and therefore the final quality, it is advisable to avoid carrying out photogrammetric work on images in this format. Although the compression ratio in this case is 1:7, which, according to previous experience, is the maximum compression with an almost unnoticeable loss of quality for current applications, the aim should be to work with the original scanning format, which was not possible in this study. Since most photogrammetry software does not allow working with ECW, we proceeded to convert ECW to TIF. This process results in a sevenfold increase in the disk space occupied by each image, from approximately 45 megabytes to 300 megabytes per image, with a total of 2.4 terabytes for the entire project.

At a first glance (Figure 4), it is already possible to observe, through the thumbnails and without going into detail, the

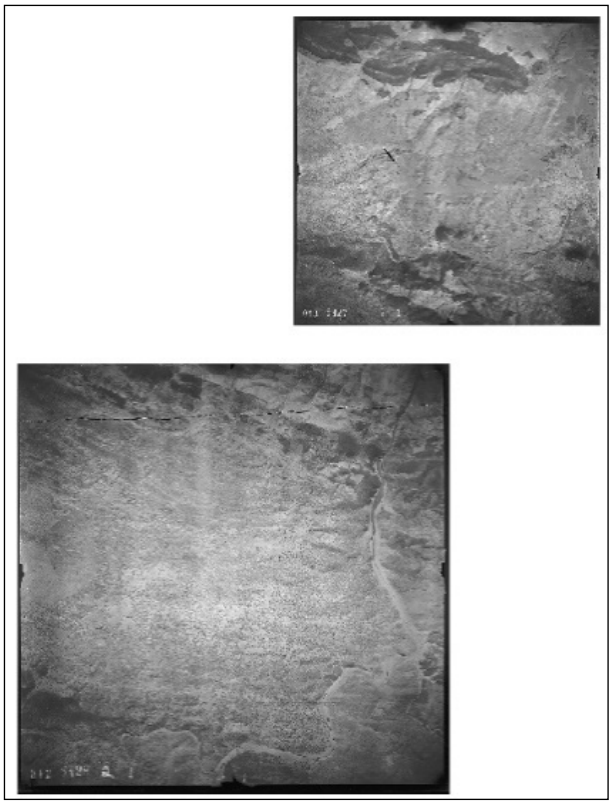

Figure 3 Different sized digital images that supposedly come from the same camera and pixel size.

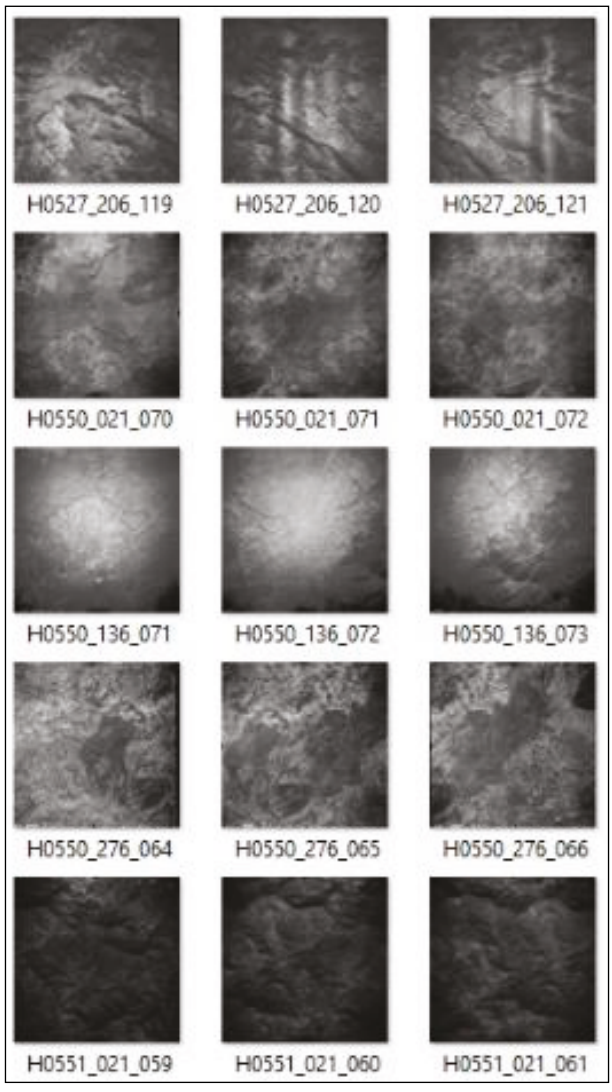

Figure 4 Radiometric problems can already be seen in the image thumbnails.

radiometric defects in the images such as: vignetting, vertical lines, halos, overexposed and underexposed images, and abrupt changes in brightness and contrast.

Looking at the images one by one, one comes to the conclusion that some of the scans were made from the paper positives and not from the original negatives; among other problems, one observes several broken positives glued with cellophane (Figure 5), which is incompatible with any precise technical process.

Figure 5 Scanned image after being repaired with cellophane.

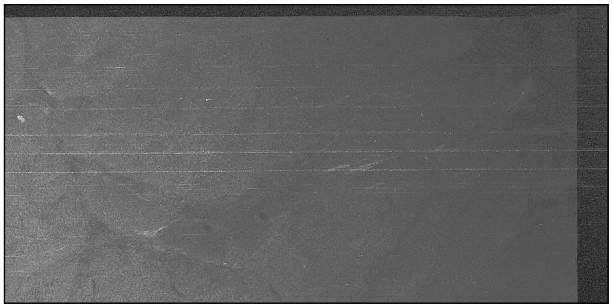

Figure 6 Lines with scratched emulsion.

Figure 7 Banding image.

Figure 8 Vignetting effect.

Scratches in the image are common (Figure 6), due to the dragging of the negative, and banding in the image, alternating between lighter and darker areas (Figure 7).

There are images where the vignetting is so strong that no information can be seen beyond the central area (Figure 8), other images appear to have ripples (Figure 9) or lack contrast (Figure 10), and there are several images with clouds and strong clouding that prevent the terrain from being seen (Figure 11).

The histograms of the images clearly show what is visually apparent, showing, underexposed, overexposed or low contrast images (Figure 12).

After image review, it was impossible to determine how many cameras were involved in the After a complete examination of the images, it was not possible

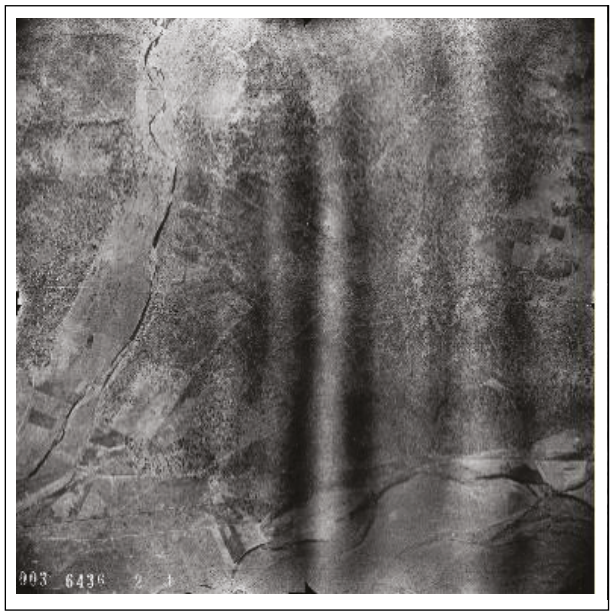

Figure 9 Image Banding or Wrinkling.

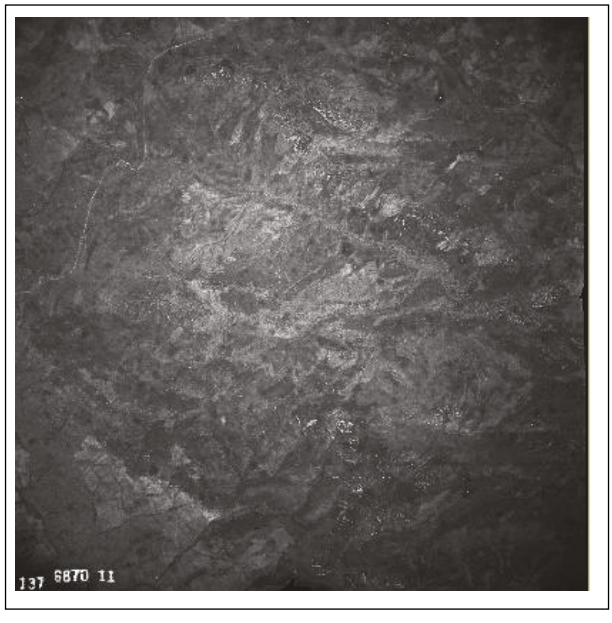

Figure 10 Low contrast.

to determine how many cameras were involved in the American flight from Extremadura, since the images were scanned by cropping this marginal information, and in the few photographs that were scanned in their entirety, there was not enough data to identify the camera with certainty. Following the recommendations of Farella et al. (2022) and Ma et al. (2020), in order to homogenise the input data, we proceeded to unify the size of the images by cropping and removing the fiducial marks, for which we performed a Photoshop automation. The purpose of this cropping is twofold: on the one hand, geometric; we eliminate the fiducials because it is not possible to measure them, as we do not have information on the camera calibration, nor can we produce a certificate from a standard model, as it has not been possible to associate each image with a camera. On the other hand, from a radiometric point of view, by cropping the image, the correlation process and the mosaicking only use the central part of the image, which significantly improves the visual aspect and eliminates a large part of the vignetting effect. However, it must be borne in mind that we are taking a risk, as the focal point of the image can now be anywhere without us having a geometric reference to determine it, and when we crop the image we are not cropping a fixed amount, as the original images were not the same size either, Instead, by an automatic process, we are left with the central square of the 10,000 × 10,000 pixels image, which means that 95% of the scanned image is taken longitudinally, but 85% transversely to the direction of flight, which can cause problems with lack of overlap between passes.

5.2 DEFINE THE WORKING BLOCKS AND GROUND CONTROL POINTS

Initially, following the recommendations of Ebadi (2006) on block size and the technical specifications of the National Plan of Historical Orthophotography of the Spanish Ministry of Public Works, it was decided to organise the work by sheets of the 1:50,000 National Topographic Map (MTN50) (Figure 13), creating 108 working blocks of 30 × 15 kilometres. However, after detailed observation of the flight lines and image overlays, it was decided to reduce the number of blocks to 78, so that some discontinuous flight strips could be linked to the transversal overlay of

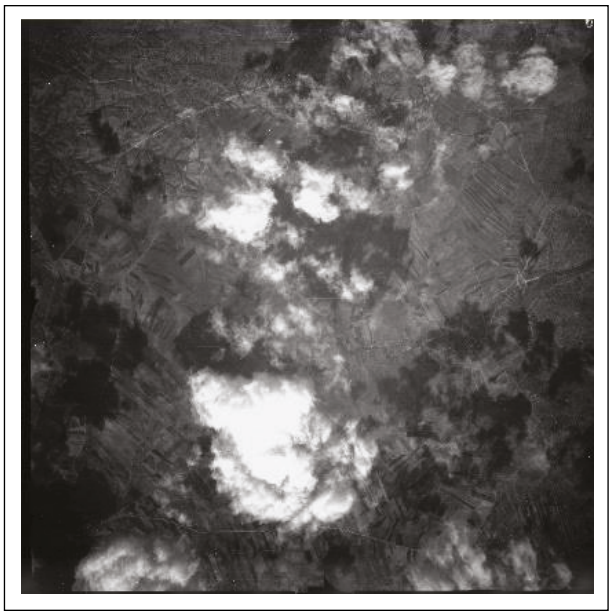

Figure 11 Clouds.

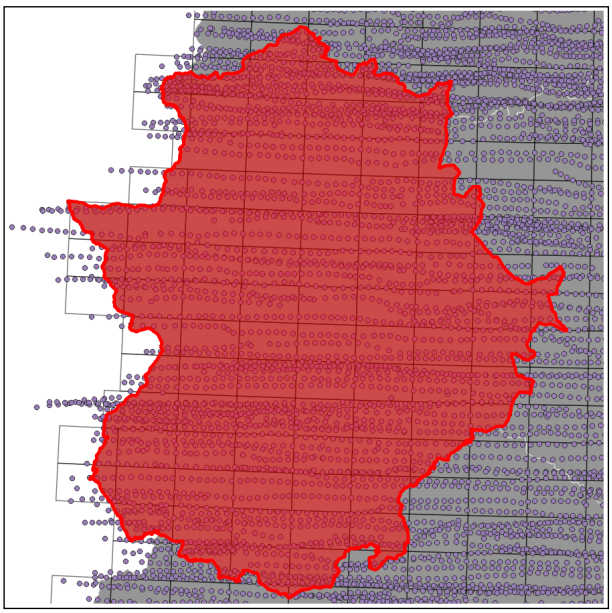

Figure 13 Photocenter of the images on the distribution of sheets of the MTN50.

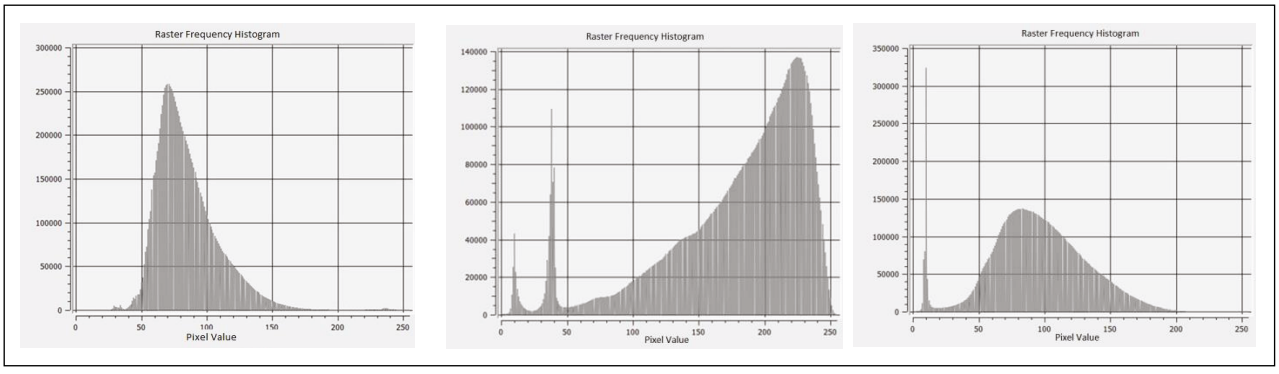

Figure 12 Histogram of three images. From left to right underexposed, overexposed, or low contrast.

the north and south lines. The average scale of the flight is 1:43,000, so each frame must cover an area of almost 10 × 10 km2. Each MTN50 sheet therefore consists of 4 passes with an average of between 7 and 10 frames, so that the number of passes would ideally be 6, the four minimum passes covering the MTN50 and one additional pass to the north and one to the south, allowing for a one-pass overlap between the aerial triangulation blocks. This implies aerial triangulation blocks of approximately 42 to 60 frames. However, a problem arises because, in many cases, and despite the inclusion of two additional strips in the block, due to the drift in the trajectory of the flight lines, this planned layout is not respected, with the appearance of significant gaps, cuts in strips or areas with an excess of frames, or even the duplication of strips (Figure 14), which means that the aerial triangulation blocks have to be modified, establishing the criterion of not interrupting the strips and linking the blocks where there are interruptions, in order to give strength to the model. It was also possible to verify that some sheets did not have complete coverage and that, a priori, it would be difficult to produce orthophotos in these areas (Figure 14). This implied the creation of 78 workspaces, in which the images of the MTN50 sheets to be orthorectified were incorporated, but it was also necessary to incorporate the north and south passes of adjacent blocks. This allowed a more robust connection between blocks than with simple GCPs and, if they were not incorporated, there was a risk that the central images would not completely cover the block.

5.3 INTERNAL ORIENTATION PROCESSES

The American flight of the A-series mainly used the Fairchild K-17 camera, the standard camera for cartographic shots of the time, 23 × 23 cm and interchangeable focal lengths of 6, 12, and 24 inches (152.4, 304.80, and 609.6 mm). The marginal information of the frame was not recorded in each exposure, but the necessary information was screen-printed afterwards in the last and first photo of the flight, which in many cases made it impossible to obtain information from the camera and flight (Quirós & Fernández 1997). The Metrogon lenses used in these cameras were later calibrated in the 1950s and showed distortions of around 120 microns. In the case of the lenses used in the 1940s, which are Metrogon type I lenses, they have a radial distortion that, according to the construction standard, should not exceed 240 microns. However, if we add to these strong distortions the geometric errors inherent in the scanning process, carried out, in some cases, from packets of very damaged frames, it is possible to expect much higher point distortions. These distortions cannot be corrected by classical photogrammetry processes; it would be necessary to implement camera self-calibration processes, which would involve numerous GCPs, and to be able to subsequently assign each of the calibrated models to the images. For this reason, it is decided to use a photogrammetric programme that makes use of SfM (Structure for Motion) technology, as has already done by several authors (Meixner 2019; Wu 2021; Yu et al. 2022; Ma, Broadbent & Zhao 2020). This process enables the orientation of images, calibration of the camera, generation of the MDS and orthophotography in a single step, with a minimal number of GCPs. Furthermore, it allows for the use of multiple cameras in a single block, as is the case with commercial programs such as Pix4D and Agisoft Metashape.

For each aerial triangulation block, an initial number of GCPs of 5 to 8 per MTN50 sheet was estimated, distributed mainly on the exterior of the block and in the interior areas, according to Kraus' recommendations (Kraus 2000), so that the total number of points planned for the entire project was 800 points, but the difficulty of locating unchanged elements in the terrain over the last 80 years became apparent when work began on locating points. Initially, the most up-to-date orthophotographs of the PNOA were used to obtain the XY coordinates, and the digital surface model obtained by LIDAR to obtain the Z coordinate, but it was quickly demonstrated that it is much easier to locate common points in flights that were closer in time, which is why the oldest possible orthophotographs were used. Even so, the number of GCPs had to be reduced, as it was impossible to locate points that had remained unchanged over time in some areas.

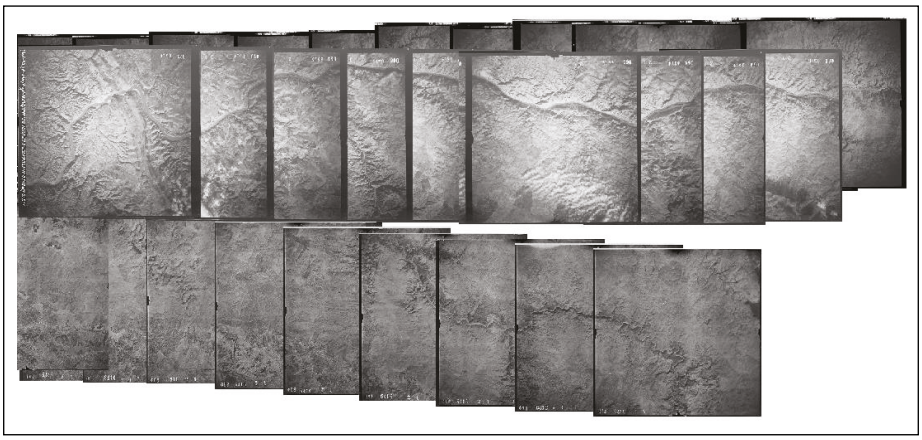

Figure 14 Some strips are duplicated and some strips lack the necessary overlap in the flight.

The elements taken as GCPs were of low geometric quality in comparison with the ground sample distance of the image, usually boundaries of farms in rural areas, walls and buildings, in any case, not very precise elements and very difficult to measure due to the state of the photographs, but it was not possible to identify points with greater definition. Each point was measured in all the photographs where it could be clearly identified, usually in 4 or 5 images (Figure 15).

6. RESULTS OBTAINED

The first works were calculated with the Pix4D programme and were blocks of 5 to 7 MTN50 sheets in an east-west direction of about 180 km in length, so as not to split the strips. (Figure 16). The number of GCPs introduced in each block varied but was always minimal, usually 4 to 6 points per MTN50 sheet, one point every 25 km. The average error in correlation was 0.76 pixels and the RMSE in terrain units was 10 metres in planimetry, but in the Z axis the RMSE goes up to 30 m, indicating a problem in the camera focal length calibration process. Looking at the RMS of the GCPs, it can be seen that the error distribution is not uniform across the block.

As predicted, the number of GCPs and their distribution, which provides reliable results for current photogrammetric flights, is insufficient for historical flights. We decided to group several blocks into a single set, increase the number of GCPs and test the results. We created an aerial triangulation block of about 40 MTN50 sheets, 180 km in the East-West direction and 100 km in the North-South direction, about 2,700 images and 207 GCPs (Figure 17), multiplying the number of images of the largest block studied in previous investigations by three, but also multiplying the number of GCPs by three (Meixner 2019).

However, the results were extremely poor, with errors well above what would be expected, although it is interesting to note that because the errors are so different and of opposite sign, the means, unlike the RSM, show unrealistic values (Table 1).

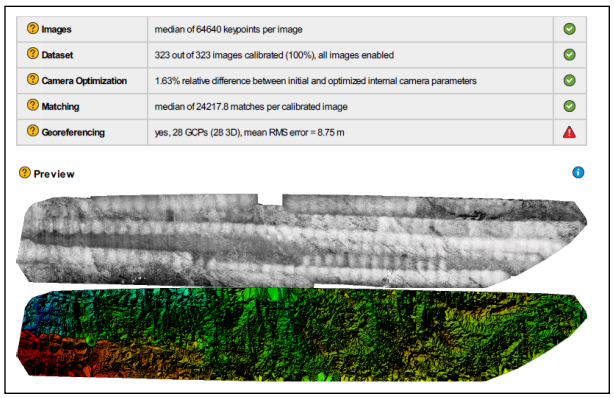

Figure 16 Summary report, block preview and generated MDS of a small block.

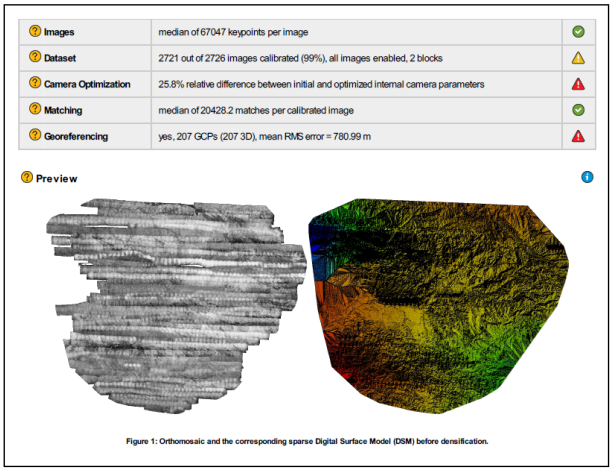

Figure 17 Summary report, block preview and generated MDS of a large block.

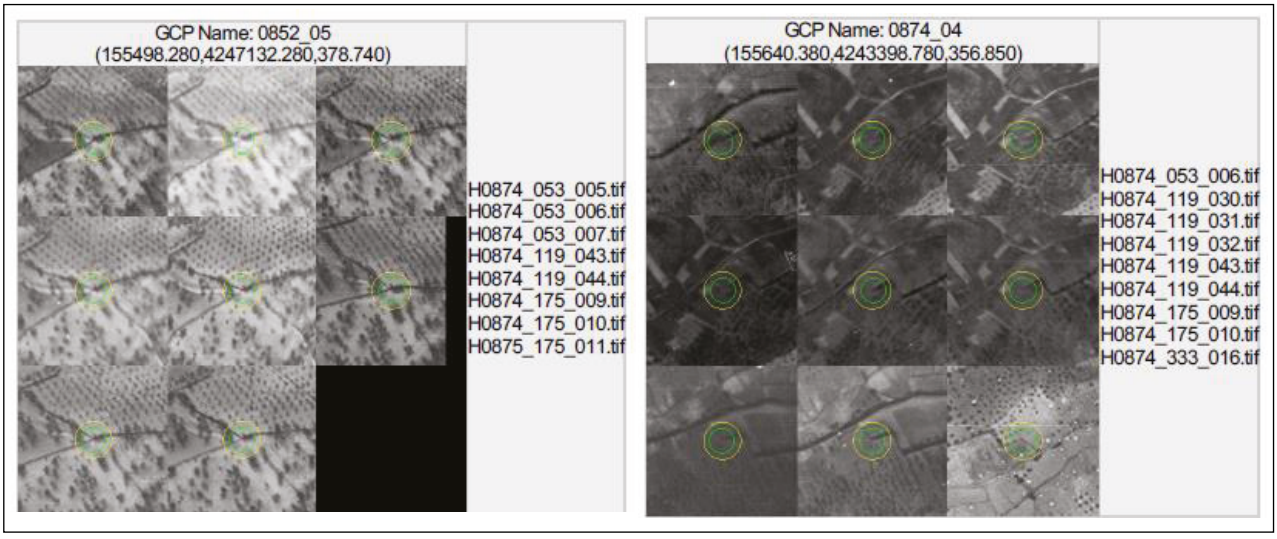

Figure 15 Identification of the same Ground Control Point on multiple images.

GCP NAME	ACCURACYXY/Z [m]	ERROR X[m]	ERROR Y[m]	ERROR Z[m]	PROJECTION ERROR [pixel]	VERIFIED/ MARKED
089705	0.100/0.200	−175.964	−19.441	48.617	1.240	7/7
089803	0.100/0.200	−121.609	6.890	128.328	0.474	5/5
089805	0.100/0.200	−43.522	−109.169	1197.336	1.168	8/8
089903	0.100/0.200	40.502	−128.445	1558.836	1.077	10/10
0899_05	0.100/0.200	109.100	−201.454	2098.839	1.273	5/5
090003	0.100/0.200	287.899	−20.691	3057.962	1.771	4/4
090005	0.100/0.200	296.065	−72.579	2992.956	0.355	3/3
0918_02	0.100/0.200	−265.289	−9.873	−422.375	0.015	2/2
0918_03	0.100/0.200	−222.517	28.630	−535.562	0.435	5/5
091805	0.100/0.200	−202.040	−30.992	136.572	0.840	4/4
0919_03	0.100/0.200	−166.555	−56.486	575.344	1.287	13/13
0919_05	0.100/0.200	−144.030	−82.729	916.786	0.780	9/9
	Mean [m]	7.86	32.835	134.506		
	Sigma [m]	231.596	215.055	1896.32		
	RMS Error [m]	231.729	217.548	1901.084		

Table 1 The different error signs compensate for the mean error while the RMS shows a much more realistic value.

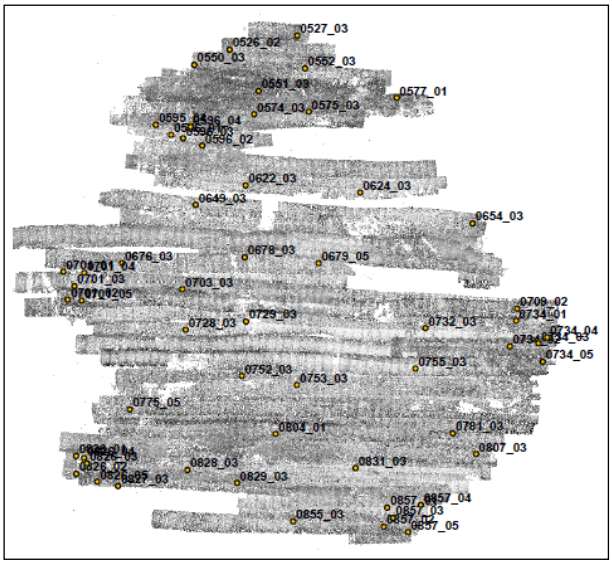

Figure 18 Footprints and GCPs.

The block calculation with Pix4D is finished and a new block is created with all the images of the project, but this time the Agisoft Metashape programme is used.

First, a calculation is made with the minimum number of GCPs, without identifying the cameras, but specifying as many cameras as there are images, so that an individual calibration is applied to each image. However, the result obtained does not manage to link many images and there are unoriented areas (Figure 18). The error in linking the images is 41 pixels, completely outside the tolerance and far from the 0.76 pixels previously obtained. However, by leaving the configuration of each camera free, the RMS in the GCPs was unrealistically low, at 0.5 m in planimetry and 1.45 m in altimetry. Previous studies with the same images, smaller and more supported blocks, obtained significantly higher values (Pérez et al. 2013).

After analysing the data, it was decided to continue with the attempt to calculate the entire block, increasing the number of GCPs and introducing some parameters of orientation and approximate camera calibration derived from the block calculation in Pix4D. It was also possible to identify two different chambers in the block from the self-calibration data provided by the initial calculation. With these parameters, the correlation error improves significantly and is 8 pixels. A total of 142 GCPs were measured, evenly distributed along the block, and the RMSE showed an unexpectedly low result of 15 cm in planimetry and 32 cm in altimetry, which is unrealistic as Ma points out in his research (Ma, Broadbent & Zhao 2020). The densification of the ground control points was continued up to 215, which improves the links between the images, but in contrast the RMSE increased to 70 cm in X, 1.6 m in Y, and 1.8 m in Z.

The real checks of the orthophotographs with linear control elements show displacements in some areas above the RMSE, so it was decided to densify some particularly conflicting areas. The number of GCPs was increased to 285 (Figure 19), the pixel correlation error value was increased to 9 pixels and the RMSE dropped to 50 cm in planimetry and altimetry.

7. CONCLUSIONS

The initial forecast of obtaining an RMSE of 1/3 of the pixel value is totally out of line with the reality of historical flights. It is not possible to achieve such accuracies when the image quality is so low and the GCPs are elements that can hardly be interpreted with an error of less than 5 metres. If the accuracy of the control and camera points is exaggerated by assigning them an extremely high value, the mathematical algorithm constrains the system and the residuals decrease in an artificial way, forcing the block to adopt an invalid geometry and reducing the RMSE drastically but introducing errors in the rectification. As Ma point out (Ma, Broadbent & Zhao 2020), an increase in the number of control points does not notably improve the final result, but rather its influence is relegated to an area very close to the new point and it is necessary to "tie up" with numerous points those blocks that do not pass the quality control. The density of GCPs needed to reduce the RMSE is uneven and depends on the orientation results. In some blocks the expected support of 15 points has been sufficient, while in other blocks more than 50 points have had to be given, the latter being more common, as the model needs high redundancy for the self-calibration processes.

Given the small number of control points that can be located, the RMSE does not represent the geometric reality of the orthophotography. The best method for checking historical imagery is visual verification on the mapping, as already deduced from the research of Ma and Buchwald (2012) (Figure 20). This makes it possible to check the orthophotography geometrically at numerous points and to ensure that each of the images that make up the mosaic has been correctly orthorectified. In any case, the geometric quality of the orthophotography using control points should be indicated as mean square error and not as median error, as it has already been seen that there are cases where the errors are compensated by creating a very low mean error, with a very high mean square error.

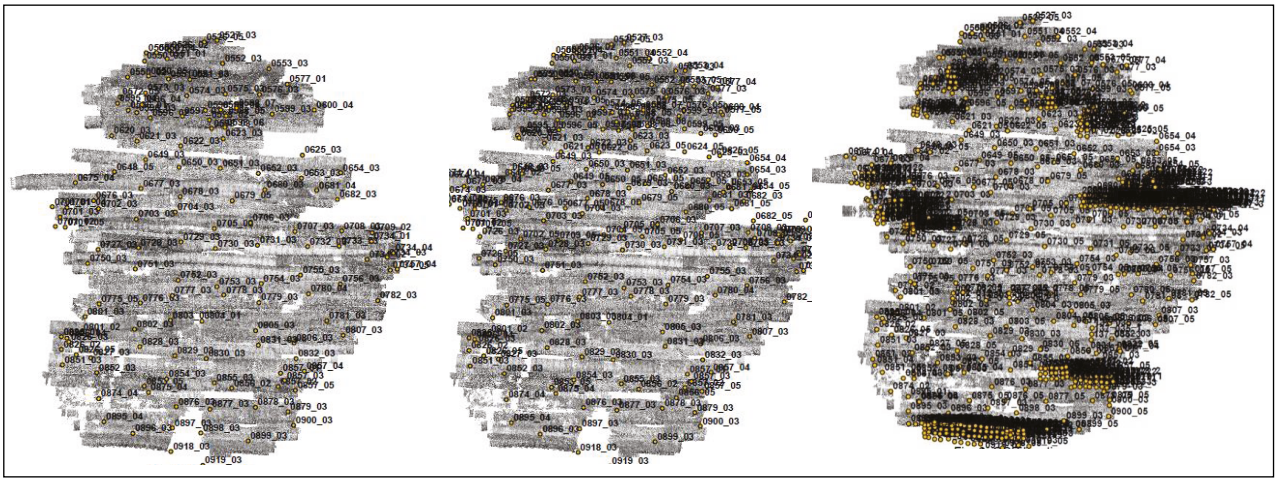

Figure 19 Footprints of oriented images and GCPs increasing from 141 to 285.

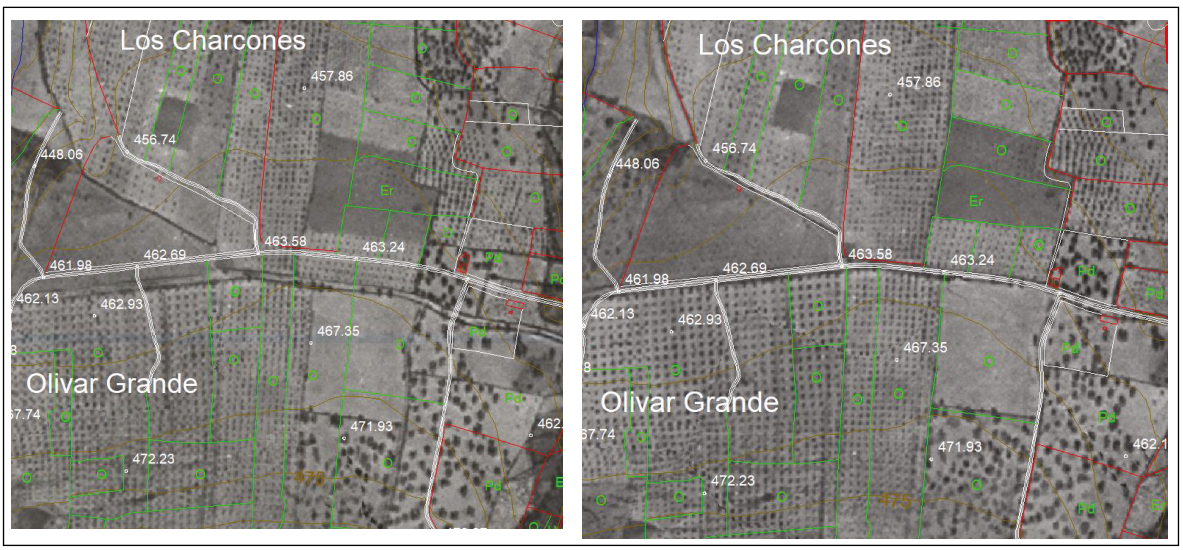

Figure 20 Linear control elements on an orthoimage deformed by excessive adjustment of the GCPs against the orthoimage with an adequate value for the accuracy of the GCPs.

With respect to the MDS, the errors in the creation of the model by correlation are very high, the processes of identification of homologous points, which causes artefacts on the orthophotographs, for this reason it was decided to work with the oldest existing MDS, which was that of the American flight series B (1954), and to update it at the time of the flight of the series A, in the areas where it was required.

Although both programmes work with SfM models, it seems that Agisoft obtains better results with large blocks, while Pix4D has obtained the best results with small blocks.

There is an interest in digitising, correcting and geo-referencing historical archives of aerial images for long-term studies of urban evolution, land use changes and environmental phenomena. Understanding these changes is crucial for assessing the long-term sustainability of urban areas and making informed decisions to ensure environmental sustainability in the future.

COMPETING INTERESTS

The authors have no competing interests to declare.

AUTHOR AFFILIATIONS

Juan-Luis Bermúdez-González orcid.org/0009-0001-3559-2507
Department of Architecture, University of Alcalá (UAH), Spain
Enrique Fernández Tapia orcid.org/0000-0001-7422-7492
Department of Architecture, University of Alcalá (UAH), Spain
Enrique Castaño Perea orcid.org/0000-0003-4332-370X
Department of Architecture, University of Alcalá (UAH), Spain

REFERENCES

Condorelli, F and **Morena, S.** 2023. Integration of 3D modelling with photogrammetry applied on historical images for cultural heritage. *Vitruvio*, 8: 58–69. DOI: https://doi.org/10.4995/vitruvio-ijats.2023.18831

Ebadi, H. 2006. *Advance analytical aerial triangulation*. Unpublished, K.N. Toosi University of Technology.

Farella, EM, Morelli, L, Remondino, F, Mills, JP, Haala, N and **Crompvoets, J.** 2022. The EUROSDR time benchmark for historical aerial images. *International archives of the photogrammetry, remote sensing and spatial information sciences*., XLIII-B2-2022, 1175–1182. DOI: https://doi.org/10.5194/isprs-archives-XLIII-B2-2022-1175-2022

Giordano, S and **Le Bris, A.** 2019. Towards fully automatic orthophoto & DSM generation. In: *EuroSDR Workshop Geoprocessing and archiving historical aerial images*, Paris, PA on 3 Jun 2019.

Giordano, S and **Mallet, C.** 2019. Archiving and geoprocessing of historical aerial images: current status in Europe. Official Publication N° 70 European Spatial Data Research.

Guoqing, Z, Jezek, K, Wright, W, Rand, J and **Granger, J.** 2002. Orthorectification of 1960s satellite photographs covering Greenland. *IEEE transactions on geoscience and remote sensing*, 40(6): 1247–1259. DOI: https://doi.org/10.1109/TGRS.2002.800240

Heisig, H, Jörg, P and **Streilein, A.** 2019. A journey through time: Digitizing, processing and publishing historical aerial imagery in Switzerland. The 1946 Showcase. In: *EuroSDR Workshop Geoprocessing and archiving historical aerial images*. Saint-Mandé, PA on 4 Jun 2019.

Hemmleb, M and **Wiedemann, A.** 1997. Digital Rectification and Generation of Orthoimages in Architectural Photogrammetry. In: *CIPA International Symposium, Göteborg, PA on 3 October 1997, IAPRS*. Vol. XXXII, Part 5C1B, pp. 261–267. In: *XVII International CIPA Symposium,* Olinda, PA on December 1999.

Kraus, K. 2000. *Photogrammetry vol. 1. Fundamentals and standard processes*. 4th ed. Bonn: Dümmler.

Ma, R. 2013. Rational Function Model in Processing Historical Aerial Photographs. *Photogrammetric engineering and remote sensing*, 79(4): 337–345. DOI: https://doi.org/10.14358/PERS.79.4.337

Ma, R, Broadbent, M and **Zhao, X.** 2020. Historical Photograph Orthorectification Using SfM for Land Cover Change Analysis. *Journal of the Indian Society of Remote Sensing*, 48(3): 341–351. DOI: https://doi.org/10.1007/s12524-019-01082-7

Ma, R and **Buchwald, A.** 2012. Orthorectify historical aerial photographs using DLT. In: *American Society for Photogrammetry and Remote Sensing Annual Conference*. Sacramento, PA on 23 March 2012, pp. 361–368.

Meixner, P. 2019. Historical Digital Orthophoto of Entire Lombardia Region. In: *EuroSDR Workshop Geoprocessing and archiving historical aerial images*. Paris, PA on 3 Jun 2019.

Nocerino, E, Menna, F and **Remondino, F.** 2018. Multi-Temporal Analysis of Landscapes and Urban Areas. In: *International archives of the photogrammetry, remote sensing and spatial information sciences*, XXXIX-B4, 5–90. DOI: https://doi.org/10.5194/isprsarchives-XXXIX-B4-85-201

Okeke, F. 2010. Review of Digital Image Orthorectification Techniques. Available at https://www.geospatialworld.net/article/review-of-digital-image-orthorectification-techniques/.

Paderes, FC, Mikhail, EM and **Fagerman, JA.** 1989. "Batch and On-Line Evaluation of Stereo SPOT Imagery". IN: *Proceedings of the ASPRS-ACSM Convention*. Baltimore, PA on 07 April 1989, pp. 31–40.

Pérez Álvarez, JA, Bascón Arroyo, FM, Crespo Pérez, FJ and **Charro Lobato, C.** 2013. Project Casey Jones, 1945–46: el vuelo histórico «fotogramétrico» de la serie A en España y sus aplicaciones cartográficas. *Mapping*, 159: 14–25.

Pinto, AT, Gonçalves, JA, Beja, P and **Pradinho Honrado, J.** 2019. From Archived Historical Aerial Imagery to Informative Orthophotos: A Framework for Retrieving

the Past in Long-Term Socioecological Research. *Remote Sensing*, 11(11). DOI: https://doi.org/10.3390/rs11111388

Quirós Linares, F and **Fernández García, F.** 1997. El vuelo fotográfico de la «Serie A». *Ería: Revista cuatrimestral de geografía*. 43: 190–8. DOI: https://doi.org/10.17811/er.0.1997.190-198

Redecker, A. 2008. Historical aerial photographs and digital photogrammetry for impact analyses on derelict land sites in human settlement areas. In: *The International Archives of the Photogrammetry, Remote Sensing and Spatial Information Sciences*, Beijin, Vol. XXXVII. Part B8.

Redweik, P, Roque, D, Marques, P, Matildes, R and **Marques, F.** 2009. Recovering Portugal aerial images repository. In: *ISPRS Hannover Workshop 2009- High-Resolution Earth Imaging for Geospatial Information*. Hannover.

Remondino, F. 2022. Geoprocessing of historical aerial images. In: *2nd EuroSDR Workshop Geoprocessing and archiving historical aerial images*. Rome, PA on 6 September 2022.

Tao, CV and **Hu, Y.** 2001a. Use of the Rational Function Model for Image Rectification. *Canadian Journal of Remote Sensing*, 27(6): 593–602. DOI: https://doi.org/10.1080/07038992.2001.10854900

Tao, CV and **Hu, Y.** 2001b. A comprehensive study of the rational function model for photogrammetric processing. *Photogrammetric engineering and remote sensing*, 67(12): 1347–1357.

Temiz, M. 2008. Rectification of digital close range images: sensor models, geometric image transformations and resampling. In: *21st ISPRS International Congress for Photogrammetry and Remote Sensing*, Beijing, cilt.37, ss.89–93.

Wu, B. 2021. Photogrammetry for 3D Mapping in Urban Areas. In: Shi, W, Goodchild, MF, Batty, M, Kwan, M and Zhang, A (eds.), *Urban Informatics*. Singapore: Springer Singapore, pp. 401–413. DOI: https://doi.org/10.1007/978-981-15-8983-6_23

Yu, J, Wu, W, Sun, J, Man, Y and **Shen, G.** 2022. A RFM adjustment method for satellite remote sensing image with Fourier compensation. *Acta Geodaetica et Cartographica Sinica*, 51(1): 127–134. DOI: https://doi.org/10.11947/j.AGCS.2021.20200429

TO CITE THIS ARTICLE:
Bermúdez-González, J-L, Fernández Tapia, E and Castaño Perea, E. 2024. New Technologies in the Processing of European Digital Heritage and Their Application to the Historical Images of the American Flight of 1944 Over Spain. *Future Cities and Environment*, 10(1): 13, 1–15. DOI: https://doi.org/10.5334/fce.252

Submitted: 18 February 2024 **Accepted:** 21 May 2024 **Published:** 17 June 2024

COPYRIGHT:
© 2024 The Author(s). This is an open-access article distributed under the terms of the Creative Commons Attribution 4.0 International License (CC-BY 4.0), which permits unrestricted use, distribution, and reproduction in any medium, provided the original author and source are credited. See http://creativecommons.org/licenses/by/4.0/.

Future Cities and Environment is a peer-reviewed open access journal published by Ubiquity Press.